nature communications

Article

https://doi.org/10.1038/s41467-024-53188-3

Unexplained high and persistent methyl bromide emissions in China

Received: 19 January 2024

Accepted: 1 October 2024

Published online: 16 October 2024

Check for updates

Xiaoyi Hu[1], Bo Yao[2,3,10] ✉, Jens Mühle[4], Robert C. Rhew[5,6], Paul J. Fraser[7], Simon O'Doherty[8], Ronald G. Prinn[9] & Xuekun Fang[1,9,10] ✉

Methyl bromide (CH_3Br) is an important ozone-depleting substance whose use is regulated under the Montreal Protocol. Quantifying emissions on the national scale is required to assess compliance with the Montreal Protocol and thereby ensure the timely recovery of the ozone layer. However, the spatial-temporal patterns of China's national CH_3Br emissions remain unclear. Here we estimate the national emissions of CH_3Br in China during 2011–2020 using atmospheric observations at 10 sites across China combined with an inversion technique (top-down) and compare those with an updated inventory of identified emission sources (bottom-up). Measured CH_3Br mole fractions are enhanced well above the background mole fractions, especially at sites in eastern China. Top-down emission estimates exceed bottom-up estimates by 5.5 ± 1.4 gigagrams per year, with the largest fraction (60%) of observationally derived CH_3Br emissions arising from underestimated or unidentified emissions sources. This study shows the potential impacts of the unaccounted emissions on stratospheric ozone depletion, with implications for the Montreal Protocol.

Global production, consumption (i.e., usage), and emissions of long-lived ozone-depleting substances (ODSs) such as chlorofluorocarbons (CFCs), halons, and carbon tetrachloride (CCl_4) have led to the depletion of the stratospheric ozone layer and contributed to global and Arctic warming[1,2]. To slow down and eventually reverse further depletion of the ozone layer, the production and consumption of these ODSs have been regulated since 1987 under the Montreal Protocol on Substances that Deplete the Ozone Layer and its Amendments[3]. Methyl bromide (CH_3Br) is an important ODS, with a lifetime of 0.8 years[4], an ozone depletion potential (ODP) of 0.6[3], and a 20-yr global warming potential (GWP) of 9[4]. CH_3Br is the single largest contributor to stratospheric bromine load, and bromine is around 60 times more efficient than chlorine in depleting ozone under current stratospheric conditions[5]. CH_3Br from natural and anthropogenic sources contributed 20% of CFC-11-equivalent emissions of all ODSs in 2020 and is projected to increase to 39% by 2100 as other ODS emissions decline[5].

Being a highly effective broad-spectrum fumigant, CH_3Br was widely used as a pest-control treatment in fumigation applications including quarantine and pre-shipment (QPS), and non-QPS uses (mainly soil, post-harvest, and structure fumigation)[5]. CH_3Br is also used as laboratory and analytical solvents and feedstocks for the manufacture of other chemicals[6]. Other sources, both natural and anthropogenic, also contribute to the atmospheric CH_3Br budget, including the oceans[7,8], biomass burning[9,10], biofuel burning[4], natural ecosystems, and certain crops[11–15]. In 1992, CH_3Br was added to Annex E of the Montreal Protocol[3]. For non-Article 5 countries (mainly developed countries), the anthropogenic production and consumption of

[1]College of Environmental & Resource Sciences, Zhejiang University, Hangzhou, Zhejiang 310058, China. [2]Department of Atmospheric and Oceanic Sciences & Institute of Atmospheric Sciences, Fudan University, Shanghai 200438, China. [3]Meteorological Observation Centre of China Meteorological Administration (MOC/CMA), Beijing 100081, China. [4]Scripps Institution of Oceanography, University of California San Diego, La Jolla, CA 92093, USA. [5]Department of Geography, University of California, Berkeley, CA 94720, USA. [6]Department of Environmental Science, Policy and Management, University of California, Berkeley, CA 94720, USA. [7]CSIRO Environment, Aspendale, Melbourne, VIC 3195, Australia. [8]School of Chemistry, University of Bristol, Bristol BS8 1TS, UK. [9]Center for Global Change Science, Massachusetts Institute of Technology, Cambridge, MA 02139, USA. [10]These authors contributed equally: Bo Yao, Xuekun Fang. ✉e-mail: yaobo@fudan.edu.cn; fangxk@mit.edu; fangxuekun@zju.edu.cn

CH_3Br were required to be frozen in 1995 and reduced by 25% in 1999, 50% in 2001, 70% in 2003, and 100% in 2005. For Article 5 countries (mainly developing countries), production and consumption were to be frozen in 2002, reduced by 20% by 2005, and eliminated by 2015, with exemptions made for QPS use[3].

China is an Article 5 country under the Montreal Protocol[3]. China's non-QPS and QPS CH_3Br consumption peaked at 3.5 gigagrams per year (Gg yr^{-1}) in 2000 and 2.1 Gg yr^{-1} in 2005, respectively (Supplementary Table 1). Although non-QPS CH_3Br consumption was scheduled to be phased out by 2015[6,16], China obtained critical use exemptions (CUEs) of approximately 0.1 Gg yr^{-1} during 2015–2018 for ginger cultivation (Supplementary Table 1), thus delaying the phase-out of non-QPS consumption to 2019.

However, China's actual national CH_3Br emissions over the last decade remain unclear. Insufficient spatial coverage of the observation site (only the Gosan (GSN) site in South Korea)[17–19] and the shortcomings of the interspecies correlation method (ISC)[17–20] have resulted in highly uncertain emission estimates and a lack of knowledge about the spatial distribution of CH_3Br emissions in China. In addition, multiyear atmospheric observation-inferred estimates of China's CH_3Br emissions are lacking. An updated and comprehensive bottom-up inventory is also necessary for comparison with the top-down estimates in China, as previous bottom-up estimates[17,21] have omitted several emission sectors, such as feedstock use[6], rice paddies[22], salt marshes[12,15], and mangrove[11].

In this work, we quantify total China's CH_3Br emissions during 2011–2020 using observations of atmospheric mole fractions of CH_3Br at ten sites across China and an atmospheric inversion method. We also develop an improved bottom-up emission inventory for known sources of CH_3Br. This study reveals that half of China's CH_3Br emissions are concentrated in the eastern provinces of China, and over half of the national emissions remain unexplained. The potential causes for these unexplained emissions and implications for stratospheric ozone depletion and the Montreal Protocol are also discussed.

Results

Higher CH_3Br mole fractions in China compared to the background atmosphere

Atmospheric mole fractions of CH_3Br were measured at 10 sites across China from 2011 to 2020 (Fig. 1, Supplementary Table 2, and Supplementary Fig. 1). We estimated the baseline (i.e., background) mole fractions at our measurement sites by selecting the lowest observed concentrations in a 90-day moving time window (see Methods). The average annual mean baselines observed during 2011–2020 ranged from 7.0 parts per trillion (ppt) at Longfengshan (LFS) to 8.2 ppt at Lin'an (LAN) (Supplementary Table 3 and Supplementary Fig. 2). These concentrations are comparable to the 7.0 to 7.8 ppt CH_3Br background mole fraction range observed at four Northern Hemisphere background sites within the Advanced Global Atmospheric Gases Experiment (AGAGE) network (https://agage.mit.edu/data/agage-data) that are at comparable latitudes to our sites in China (24.0° N–47.1° N): Mace Head site in Ireland (MHD hereafter, 53.3° N, 9.9° W), Trinidad Head site in California, USA (THD hereafter, 41.1° N, 124.2° W), Gosan site on Jeju Island, South Korea (GSN hereafter, 33.3° N, 126.9° E), and Ragged Point site in Barbados (RPB hereafter, 13.2° N, 59.4° W). The background mole fractions at those four AGAGE sites were determined by using AGAGE's statistical algorithm which extracted the background observations by applying a second-order polynomial to the daily minima over a 120-day moving time window[23]. To ensure comparability, we verified that the background mole fractions estimated using AGAGE's method and this study's method were consistent (Supplementary Fig. 3).

Enhanced mole fractions above baseline values at each of the ten Chinese sites reflect emissions in China and other Asian countries surrounding China. These pollution events showed spatial heterogeneity among the ten Chinese sites, with the highest average annual mean enhanced mole fraction of 9.9 ± 1.4 ppt observed at the LAN site in eastern China and the lowest of 0.6 ± 0.8 ppt observed at the Mount Waliguan (WLG) site in northwest China (Supplementary Table 3 and Supplementary Fig. 2). The higher enhancements in the eastern provinces of China indicate potentially stronger CH_3Br emissions from this region (see discussion in the next section).

Persistent CH_3Br emissions in China after the 2015 phase-out

The measurements at these sites were sensitive to emissions in most of China (Fig. 1 and Supplementary Fig. 1), such that national CH_3Br emissions can be quantified using an inversion of the atmospheric measurements (see Methods). This study improves on previous studies by using more sites within China's borders, allowing a better quantification of national emissions. CH_3Br emissions in China averaged 9.2 ± 1.4 Gg yr^{-1} during 2011–2020 (Fig. 2a). Emissions showed interannual variations but no significant trend (slope = 0.16 ± 0.15 Gg yr^{-1}, $p = 0.33$), with a maximum of 10.5 ± 1.4 Gg yr^{-1} in 2014 and a minimum of 6.2 ± 1.1 Gg yr^{-1} in 2012 (Fig. 2a). These results are generally consistent with national emissions estimated by the interspecies ratio method (Supplementary Fig. 4), although prior results were single year estimates from the beginning of this study or earlier: ~5.5 ± 2.0 Gg yr^{-1} in 2008[18,19]. Based on the recently established long-term observation network in China, this study addresses the magnitude and 2011–2020 trend of national CH_3Br emissions in China.

We identified eastern China (enclosed by red lines in Fig. 2b, including the 11 provinces of Anhui, Beijing, Hebei, Jiangsu, Liaoning, Shandong, Shanghai, Tianjin, Zhejiang, Fujian, and Guangdong) as the hotspot for emissions (Fig. 2b and Supplementary Fig. 5). The CH_3Br flux (emission rate per unit area) in eastern China was eight times that of the rest of China (4.0 and 0.53 kg km^{-2} yr^{-1}, respectively) from 2011 to 2020 (Fig. 2b). Even though the area of eastern China accounts for only 12.5% of China's total area, their emissions contributed about 52% (4.8 Gg yr^{-1}) of total emissions. As shown in Supplementary Table 4, the top five CH_3Br emitting provinces were Jiangsu (0.76 ± 0.16 Gg yr^{-1}), Shandong (0.74 ± 0.12 Gg yr^{-1}), Zhejiang (0.72 ± 0.23 Gg yr^{-1}), Anhui (0.66 ± 0.19 Gg yr^{-1}), and Guangdong (0.50 ± 0.17 Gg yr^{-1}), contributing approximately 40% of China's national CH_3Br emissions. For comparison, these five provinces represent 7.3% and 32% of China's total area and population, respectively. As shown in Supplementary Fig. 4, the emission estimates for eastern China in this study are consistent with those derived from observations at the GSN site in South Korea and the interspecies ratio method by Choi et al.[17].

Accounting of CH_3Br emissions from known sources in China

National bottom-up CH_3Br emissions in China estimated in this study were 3.7 ± 0.2 Gg yr^{-1} on average during 2011–2020 (Fig. 3 and Supplementary Table 5). These were, on average, 2.8 ± 0.2 Gg yr^{-1} significantly higher than the fumigation sector estimates alone (the sum of QPS and non-QPS emissions based on CH_3Br consumption data reported to the United Nations Environment Programme (UNEP)) and 1.2 ± 0.2 Gg yr^{-1} significantly higher than the total estimate (fumigation plus three non-fumigation sectors) by Choi et al.[17]. CH_3Br emissions from fumigation (QPS + non-QPS) sectors were about 2.0 Gg yr^{-1} (54% of the total bottom-up emissions) on average during 2011–2020. Non-QPS fumigation emissions in this study (0.07 Gg yr^{-1}) were consistent with amounts reported to UNEP (0.06 Gg yr^{-1}), while the QPS emissions (1.96 Gg yr^{-1}) were higher than reported (0.91 Gg yr^{-1}). QPS emissions that are primarily associated with the import/export shipping industry contributed over 90% of the total fumigation emissions (Fig. 3). China's port cargo throughput is concentrated in eastern China provinces (Supplementary Table 6 and Supplementary Fig. 6); thus, QPS emissions associated with shipping may account for some of the emission hotspots of eastern China.

Compared with Choi et al.[17], seven additional sectors were considered in this study, including non-fumigation anthropogenic sectors

https://doi.org/10.1038/s41467-024-53188-3

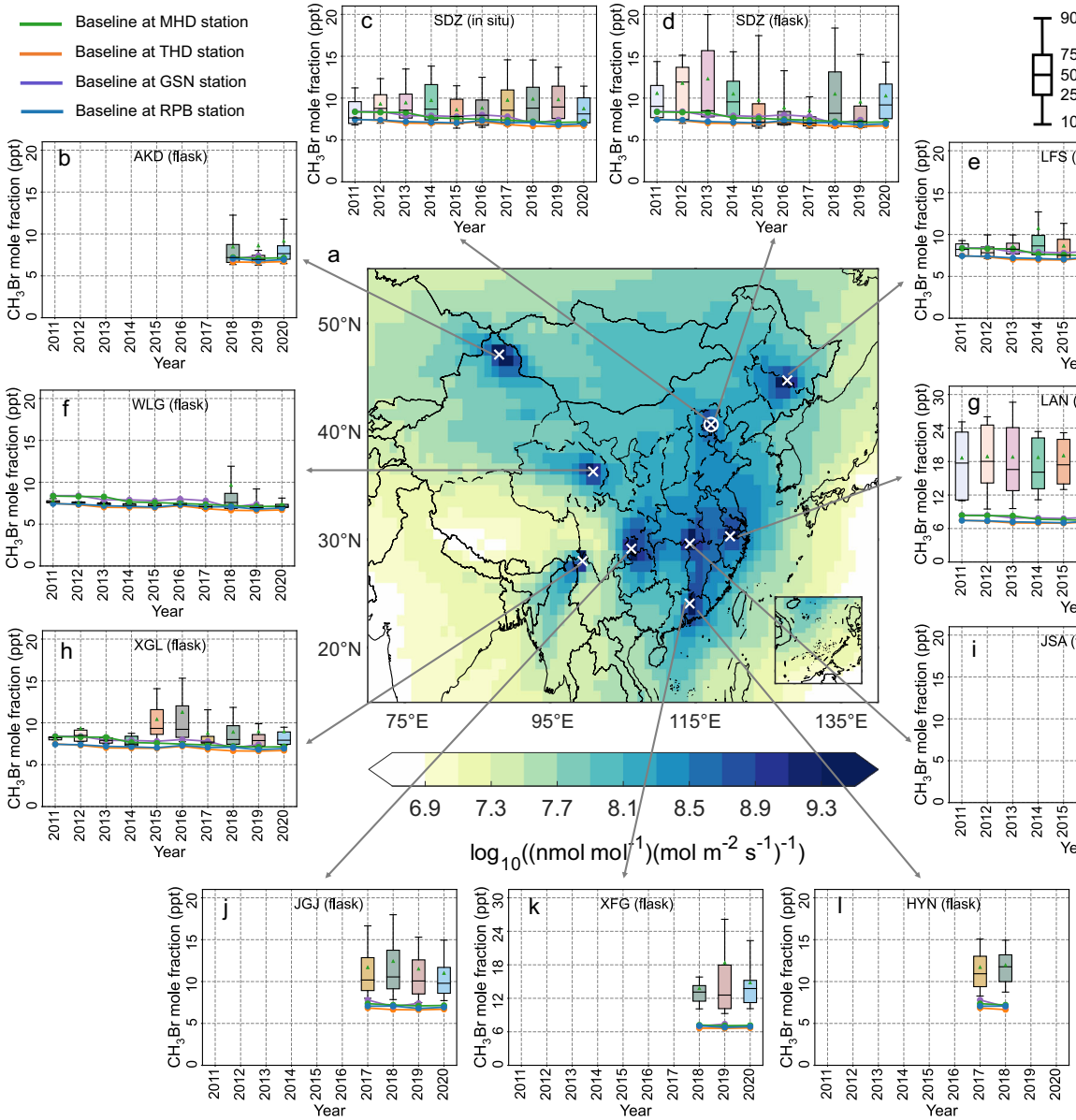

Fig. 1 | The sum of annual averaged footprints from each site in 2020 and atmospheric mole fractions of CH_3Br observed at ten sites in China during 2011–2020. a The locations (white cross) and the sum of annual averaged footprints from each site in 2020. Darker colors indicate higher emission sensitivity. Emissions throughout most of China can be constrained by measurements at the ten sites. **b**–**l** Box-and-whisker plots of CH_3Br atmospheric mole fractions at each site during 2011–2020. The box and whisker plots depict the 10th, 25th, 50th, 75th, and 90th percentiles of the CH_3Br mole fractions. The green, orange, purple, and blue lines represent the annual mean background mole fractions of CH_3Br at Mace Head (MHD), Trinidad Head (THD), Gosan (GSN), and Ragged Point (RPB) sites, respectively (for comparison only).

(feedstock[6,24], solvents[24–26], CH_3Br industrial production[24]) and terrestrial ecosystem sectors (rice paddies[13,22], salt marshes[12,15], mangroves[11], and fungi[27,28]). CH_3Br emissions from these seven sectors reached 1.0 ± 0.1 Gg yr^{-1} on average during 2011–2020, which accounted for 26% of the total bottom-up emissions and were equal to the sum of fumigation use (QPS and non-QPS sectors) emissions based on CH_3Br consumption data reported by China to UNEP (Fig. 3c). Thus, the addition of these seven sectors substantially improves the bottom-up estimates of CH_3Br emissions in China.

Unexplained high emissions of CH_3Br from China and their potential causes

In total, our bottom-up emission estimates of 3.7 ± 0.2 Gg yr^{-1} remain 5.5 ± 1.4 Gg yr^{-1} lower than our top-down estimates (9.2 ± 1.4 Gg yr^{-1}) on average during 2011–2020 (Fig. 4 and Supplementary Table 7). The gap between our top-down and bottom-up emissions estimates is large, amounting to approximately 60% of the top-down estimates. The unexplained CH_3Br emissions in China may be attributed to three possible causes.

First, multiple instances of illegal production and sales were reported between 2010 and 2014 in multiple provinces[29–34] (magenta triangles shown in Fig. 2b). Although the above-mentioned activities were punished and reported, multiple instances of illegal production still occurred in 2020 in the Shandong Province[35,36] (yellow dots shown in Fig. 2b). The proportion of emissions from this source to the total unexplained emissions is unclear.

Second, known terrestrial sources of CH_3Br may be underestimated. The emission fluxes of CH_3Br from terrestrial sources (such as salt marshes, rice paddies, and rapeseed) vary with temperature[37], Br content of the soil[22], and plant types[38]. However, measurements of

https://doi.org/10.1038/s41467-024-53188-3

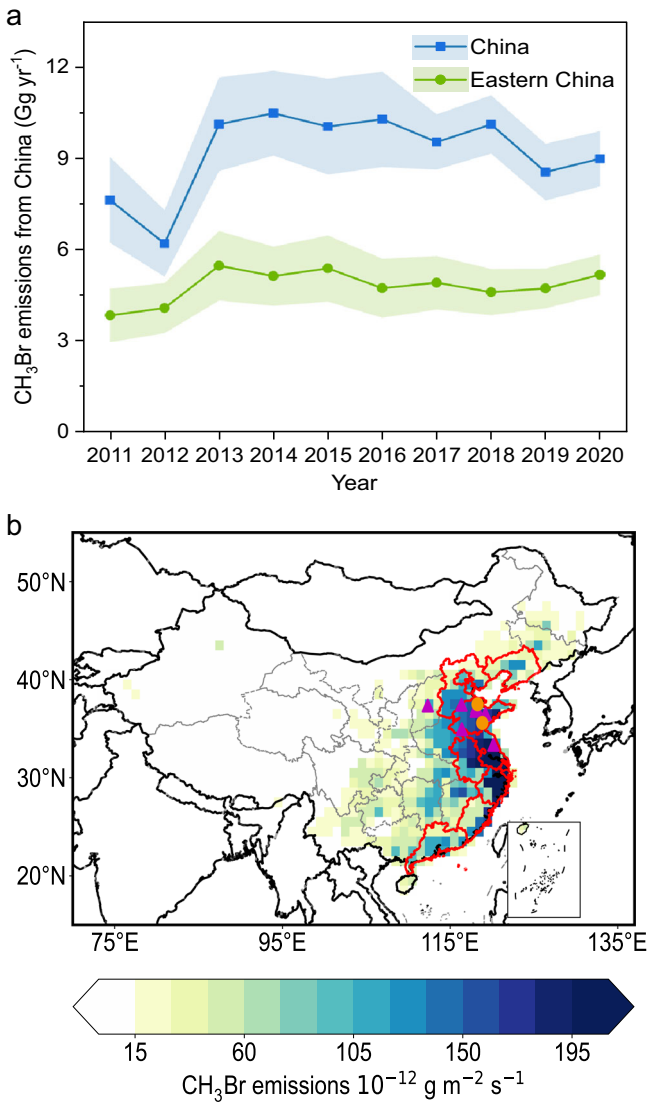

Fig. 2 | CH_3Br emissions inferred from atmospheric observations and inversion. **a** CH_3Br emissions in all of China and eastern China. The shaded area represents 1-sigma uncertainties. **b** Spatial distribution of average CH_3Br emissions during 2011–2020. Eastern China (enclosed with red lines) shows the highest emission rate per unit area in China. The hatched areas represent regions to which our observations have low sensitivity and are excluded from the emission estimates in this study. The magenta triangles and yellow dots represent the locations with reported illegal productions and sales of CH_3Br in China between 2010 to 2014[29–34] and in 2020[35,36], respectively.

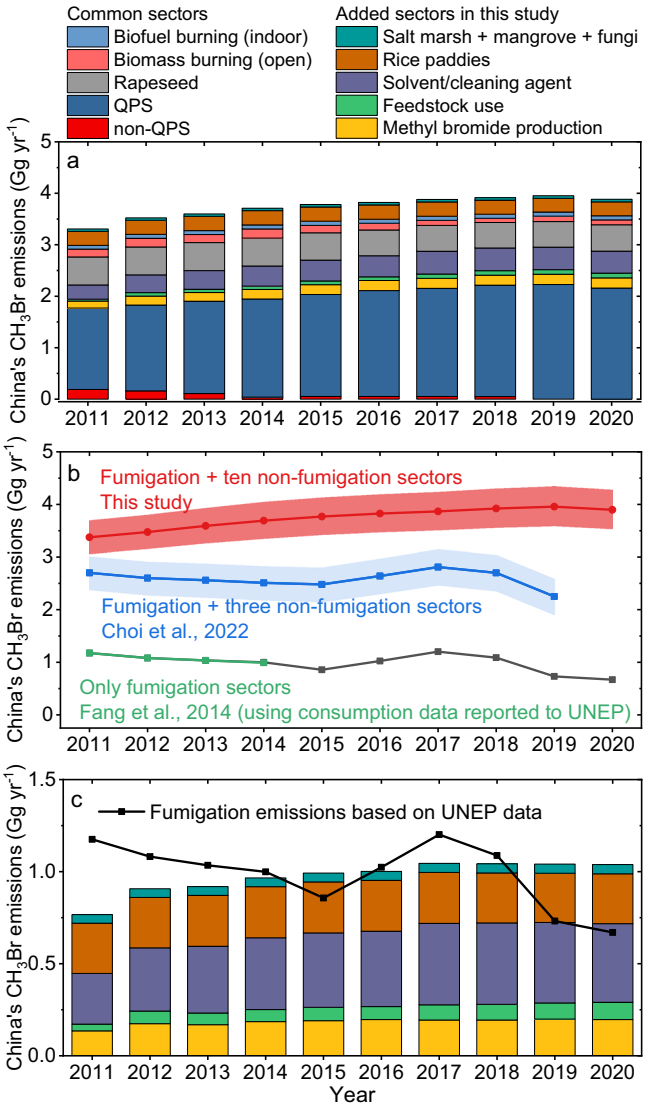

Fig. 3 | Comparisons of bottom-up inventories of CH_3Br emissions from China during 2011–2020. **a** Total bottom-up emissions of CH_3Br in China during 2011–2020. The stacked bars represent the emissions from each sector included in this study. **b** Comparisons of total bottom-up estimates between this study and Choi et al.[17], Fang et al.[21], and fumigation emissions including quarantine and pre-shipment (QPS) and non-QPS sector based on consumption data reported to the United Nations Environment Programme (UNEP). **c** Emissions from seven added sectors in this study. The stacked bars represent the emissions from seven added emission sectors in this study; combined, they are similar in magnitude to the fumigation emissions based on UNEP consumption data. Note that fumigation includes QPS and non-QPS applications.

CH_3Br emission fluxes from these sources are sparse[27], limiting the accuracy of estimates for emissions from these sources. Representative CH_3Br flux measurements in China need to be conducted in the future to better quantify the emissions from these terrestrial sources. Although coastal ocean waters are also a source of CH_3Br (the open ocean is a net sink of CH_3Br)[39], China's CH_3Br emissions from coastal ocean waters are estimated at 0.05 (0.01–0.15) Gg yr^{-1} based on the area of China's coastal ocean waters[40] and measured emission flux rates[39], so coastal ocean waters are unlikely to be major contributors to the large unexplained sources observed here.

Third, it is likely that additional sources remain to be identified. New emission sources of CH_3Br are still being discovered in recent years, such as baking discovered in 2016[41] and copper-based pesticides discovered in 2022[42], reflecting our incomplete understanding of CH_3Br sources. However, the emission contribution from baking is negligible (about 0.2 Gg yr^{-1} globally[41]). Using China's $CuSO_4$ consumption (Supplementary Table 8) and the relationship between copper (II) amendments and CH_3Br emissions reported by Jiao et al.[42], China's emission from this sector is likely also negligible (0.01 ± 0.004 Gg yr^{-1}). Note that due to the lack of China's $CuSO_4$ consumption for pesticide use, we use total $CuSO_4$ consumption to estimate emissions from this sector (data and calculation shown in Supplementary Table 8). Therefore, the missing source in China cannot be well explained by these newly-identified sources but may be explained by sources yet to be identified. The emission hotspots identified via our inverse modeling may provide some implications for future work on identifying new sources. In summary, unreported production, emissions from known natural sources (if underestimated),

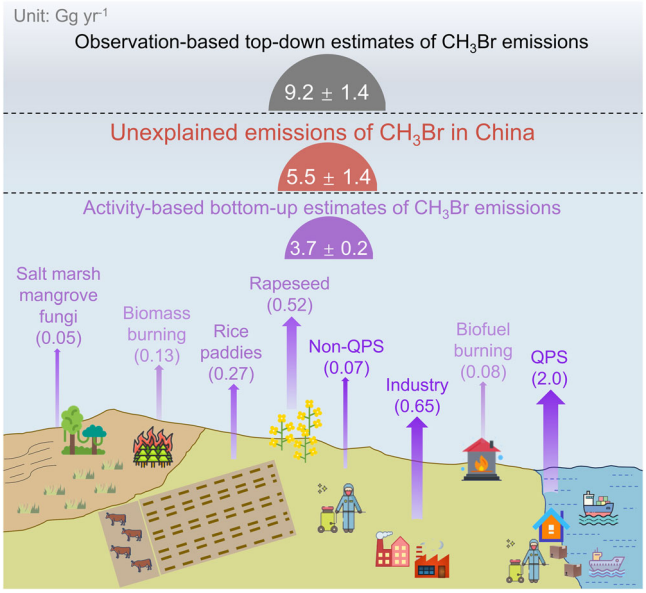

Fig. 4 | The large gap between China's top-down and bottom-up emission estimates. The bottom-up inventory depicts our best attempt at estimating all known CH_3Br emissions in China and is compared with our top-down estimates to depict the gap in emissions estimates. The dark purple arrows represent anthropogenic production and consumption sources (industry sources include CH_3Br production, feedstock use, and solvent/cleaning agent use); the light purple arrows represent the combustion sources (open biomass burning and indoor biofuel burning), and the purple arrows represent terrestrial ecosystem sources (salt marshes, mangroves, fungi, rapeseed, and rice paddies). The thickness of the arrow represents the relative contribution of each emission sector to the total bottom-up inventory.

and unidentified new sources may contribute to China's large missing source of CH_3Br.

Discussion

The importance of emissions of CH_3Br relative to other ODSs in China for stratospheric ozone depletion is increasing. The ODP-weighted emissions (CFC-11-eq emissions) of CH_3Br in China estimated in this study amounts to 5.5 ± 0.78 CFC-11-eq Gg yr^{-1}, nearly 80% of the unexpected emissions of CFC-11 (one of the major first generation ODSs; 7.0 ± 4.0 Gg yr^{-1}) in eastern China during the 2014–2017 period[43,44]. Since the CFC-11 emissions reduced rapidly between 2017 and 2019[44], China's national CH_3Br emissions surpassed eastern China's CFC-11 emissions (5.0 ± 1.0 Gg yr^{-1}) in 2019, and the gap is expected to have grown larger beyond 2019. Moreover, CH_3Br emissions in all of China in 2020 were several times higher than the emissions of other major ODSs; e.g., they were 13 times the emissions of dichlorodifluoromethane (CFC-12, 0.43 CFC-11-eq Gg yr^{-1}), 0.9 times the emissions of chlorodifluoromethane (HCFC-22, 6.2 CFC-11-eq Gg yr^{-1}), 1.7 times the emissions of 1,1-dichloro-1-fluoroethane (HCFC-141b, 3.2 CFC-11-eq Gg yr^{-1}), and 37 times the emissions of 1-chloro-1,1-difluoroethane (HCFC-142b, 0.15 CFC-11-eq Gg yr^{-1})[45].

If the unaccounted emissions of CH_3Br in China continue to 2050, they will amount to an integrated ozone depletion (IOD) of approximately 20 DU years (see calculations in Methods). Note that this calculated IOD depends on the future evolution of CH_3Br emissions. It is important to figure out how much of the unaccounted emissions of CH_3Br are anthropogenic and to determine their future evolution in order to assess compliance with the Montreal Protocol. Unpermitted usage and sales of CH_3Br occurred both in China as well as other countries, such as from 2013 to 2015 in the United States[46]. Illegal production, trade, and even smuggling[47] are transboundary issues that affect the efficacy of the Montreal Protocol and may contribute to global discrepancies in source data. The impacts on stratospheric ozone depletion are expected to be larger than 20 DU years if unidentified sources in other countries are also significant.

In summary, the largest fraction of the total CH_3Br emissions in China remains unexplained, which poses challenges to the scientific understanding of the CH_3Br budget. In future studies, acquiring accurate production and consumption data and identifying new sources will be critical to minimize the gap between top-down and bottom-up emission estimates, and to safeguard the ozone layer recovery.

Methods

Sampling and analysis

Atmospheric mole fractions of CH_3Br were measured at ten sites across China from 2011 to 2020: Akedala (AKD), Heyuan (HYN), Jiangjin (JGJ), Jinsha (JSA), Lin'an (LAN), Longfengshan (LFS), Mount Waliguan (WLG), Xinfeng (XFG), Shangri-La (XGL), and Shangdianzi (SDZ). The detailed information on these ten sites is summarized in Supplementary Table 2. These sites were located more than 20 km from the nearest industrial and densely populated areas in order to sample air masses carrying regional emission signals[48–51].

Weekly or daily sampling was conducted at all ten sites (Supplementary Table 2). The same sampling and analysis methods were used at the ten sites, as described in detail in previous studies[48,50]. Air samples were pumped by a membrane pump (KNF-86, KNF Neuberger, Germany) from the tops of the sampling towers through a sampling tube (10 mm OD Synflex tubing, Eaton, USA) into 3 L stainless steel canisters (X23-2N, LabCommerce, Inc., USA)[50]. All the flask air samples were sent to the central laboratory at the Meteorological Observation Centre in Beijing for analysis within one month[49,50]. At each site, pairs of parallel samples were collected concurrently for quality assurance[49,50]. Additionally, at the SDZ site, an in situ sampling and analysis system was operated during 2011–2020. All the flask and in situ samples were analyzed by a "Medusa" gas chromatographic system with a mass spectrometric detector (Agilent 6890/5975B, USA)[50]. To detect and correct for drift in detector sensitivity, each air sample measurement from canisters was bracketed by a reference gas (real-air working standard) measurement[50]. Atmospheric measurements of CH_3Br are linked to AGAGE standard scales[50,52], and the dry mole fractions of CH_3Br were reported using the Scripps Institution of Oceanography 2005 (SIO-2005) calibration scale[50]. We performed a stability test for CH_3Br as long as 112 days, and the recoveries were 101%, 101%, 102%, 101%, 102%, and 98% for Days 9, 18, 41, 65, 90, and 112, respectively. For each tested day, we analyzed four SS flasks and took the average. There was no significant drift for CH_3Br measurements, with a standard deviation of the four flasks being 1–2% (Supplementary Table 9). The measurement precision of CH_3Br was 1% for measurements on flask samples and 0.6% for SDZ in situ measurements[50]. All observation data used in the emission inversion are shown in Supplementary Fig. 7.

As shown in Fig. 1 and Supplementary Fig. 1, the total annual average emission sensitivity data (derived from FLEXPART backward simulations, see next section) of these sites (sum of averaged footprints every three hours for all sites with measurements in that year) exhibit a high spatial coverage for all of China, which ensures that the national total emissions in China can be constrained by observations at these sites. Nonetheless, adding more observational sites in regions that currently do not have sites, should help to better constrain regional emissions in the future.

FLEXPART-based Bayesian Inversion of emissions

In this study, the Bayesian inversion algorithm and FLEXPART ("FLEXible PARTicle dispersion model") atmospheric transport model were used to estimate national CH_3Br emissions in China. This

framework was well-established and described in detail in previous studies[48,49,53]. FLEXPART is a Lagrangian transport and dispersion model (http://www.flexpart.eu/) that has been widely used in simulating the transport of various atmospheric species[54,55]. The three-hour temporal resolution and 1° × 1° global meteorological data from the European Centre for Medium-Range Weather Forecasts (ECMWF) was used to drive the FLEXPART model. To obtain the source-receptor relationship matrix (SRRs, also called "emission sensitivity" or "footprint", in units of $m^2\ s\ g^{-1}$), in the FLEXPART model, 40k virtual particles were released from the location of each observation site in a three-hour interval, and the model was run backward for 20 days for each atmospheric observation[48,49]. This matrix relates emission fluxes at the source to atmospheric mole fractions measured at the receptor (measurement site)[48,49]. During the 20-day backward simulation, the fraction of chemical loss to emission resulting from CH_3Br lifetime (0.8 years) is approximately only 1.7% (1-exp(−5/(0.8 × 365))) considering that the enhancements measured at observation sites are typically influenced by emissions within a five-day transport of an air mass[54]. A previous study demonstrated that the inversion results of $CHCl_3$ (lifetime = 0.4 years) changed by only 1% when chemical losses were included in the simulation[53]. Thus, the chemical losses of CH_3Br were not considered in our backward simulation. Under the Bayesian inversion framework, we obtained the optimal posterior emission by minimizing the following cost function as Eq. (1):

$$J(x) = \frac{1}{2}(\mathbf{x}-\mathbf{x_a})^{\mathrm{T}}\mathbf{S}_a^{-1}(\mathbf{x}-\mathbf{x_a}) + \frac{1}{2}\left(\mathbf{y^{obs}}-\mathbf{Hx}\right)^{\mathrm{T}}\mathbf{S}_o^{-1}\left(\mathbf{y^{obs}}-\mathbf{Hx}\right) \quad (1)$$

The optimal $\mathbf{x}$ is solved at $\nabla_x J(x) = 0$ as shown in Eqs. (2) and (3):

$$\mathbf{x} = \mathbf{x_a} + \mathbf{S}_a\mathbf{H}^{\mathrm{T}}\left(\mathbf{H}\mathbf{S}_a\mathbf{H}^{\mathrm{T}} + \mathbf{S_o}\right)^{-1}(\mathbf{y^{obs}} - \mathbf{Hx_a}) \quad (2)$$

$$\mathbf{S}_b = \left(\mathbf{H}^{\mathrm{T}}\mathbf{S}_o^{-1}\mathbf{H} + \mathbf{S}_a^{-1}\right)^{-1} \quad (3)$$

where $\mathbf{x}$ is the state vector of the posterior emission strengths in each grid box, $\mathbf{y^{obs}}$ is the observed enhanced mole fraction (observations minus baselines), $\mathbf{x_a}$ is the prior emission vector, $\mathbf{H}$ is the emission sensitivity matrix derived from the FLEXPART backward simulation, $\mathbf{S}_a$ is the prior emission error covariance matrix, $\mathbf{S}_b$ is the posterior emission error covariance matrix, and $\mathbf{S_o}$ is the observational error covariance matrix.

Choi et al.[17] estimated CH_3Br emissions from eastern China at 4.1 ± 1.3 Gg yr^{-1}. Therefore, we used a constant prior for China's CH_3Br emissions of 5 Gg yr^{-1} during the study period and disaggregated the total emissions by population spatial distribution (Gridded Population of the World: Future Estimates, 2020). To ensure that our inversion estimates were not sensitive to the choice of the prior emission estimate, we scaled the prior emissions by factors of 0.5 and 1.5 and then repeated the inversion (Supplementary Fig. 8a). Because of the lack of uncertainty in the gridded prior emissions, we set the prior emission uncertainty in each grid to 100%, 150%, and 200% of the corresponding emissions[48,49]. The final posterior emission was the ensemble result of nine inversions (three prior emission fields × three prior emission uncertainties)[48,49]. For the flask sampling sites, background mole fractions were estimated as the lower value of (1) the lowest measurement in the 90-day moving window and (2) the latitude-direction linearly interpolated value between the monthly mean background value at the Ragged Point site (RPB, 13.17° N, 59.43° W) and Mace Head site (MHD, 53.33° N, 9.9° W)[48,49]. In most cases, the lowest measurement in the 90-day moving time window was chosen as the baseline. Additionally, we tested our inversion using the same baseline calculation method mentioned above but incorporated the monthly mean background value at the Trinidad Head site (THD; 124.2° W, 41.1° N) instead of the MHD site (Supplementary Fig. 8b). For the SDZ in situ site, background mole fractions were estimated using the approach of Stohl et al.[54], which selects the lowest 25% of the observations in a 30-day moving time window and then subtracts prior simulated enhancements. Observational errors are represented by one-sigma standard deviations of all observation data in a year at a site[48,49]. To eliminate the temporal correlation of high-frequency measurements at the SDZ in situ site, the daily averages of measurements were used in our inversion[48,49]. The observational error covariance matrix $\mathbf{S_o}$ is a diagonal matrix, with diagonal elements representing the square of the observation error.

Bottom-up emission inventory of China's CH_3Br

We estimated China's CH_3Br emissions from four sectors: (1) fumigation, (2) CH_3Br production and non-fumigation, (3) combustion, and (4) terrestrial ecosystems. The emissions from each sector were calculated as follows:

In terms of the fumigation use sector, CH_3Br has been used extensively worldwide as a pest-control fumigant since the 1950s[6]. Fumigation uses include quarantine pre-shipment (QPS) and non-QPS applications. The emissions calculation equation is as Eq. (4):

$$E_{fumigation,t} = C_{non-QPS,t} \times EF_{non-QPS} + C_{QPS,t} \times EF_{QPS} \quad (4)$$

where $E_{fumigation,t}$ is the emissions (Gg yr^{-1}) of the fumigation sector in year t, $C_{non-QPS,t}$ and $C_{QPS,t}$ are the consumption (Gg yr^{-1}) of the non-QPS and QPS uses in year t, respectively, and $EF_{non-QPS}$ and EF_{QPS} are the emission factors of the non-QPS and QPS uses, at 65% and 84%, respectively[3]. The consumption data for non-QPS and QPS are listed in Supplementary Table 10.

In terms of CH_3Br production and non-fumigation use sector, considering the possibility of CH_3Br leakage from industrial production, similar to the leakage calculations during CCl_4[56] and CH_2Cl_2[51,57] production, we calculated the emissions from the CH_3Br production subsector. In addition to fumigation uses, some CH_3Br has been used for non-fumigation uses, including two subsectors: feedstock uses[6] in the organic synthesis industry and solvents/cleaning agents[26]. The emissions from these three subsectors were calculated as Eq. (5):

$$E_{production\ and\ non-fumigation,t} = \sum_{i=1}^{3} C_{i,t} \times EF_i \quad (5)$$

where $E_{production\ and\ non-fumigation,t}$ are the emissions (Gg yr^{-1}) from the CH_3Br production and non-fumigation use sectors in year t, i represents the number of sectors, C_i is the consumption (Gg yr^{-1}) of feedstock use, solvent/cleaning agents, or production of CH_3Br in year t. The consumption and production data are listed in Supplementary Table 10. EF_i is the emission factor for the three subsectors. The emission factor was 4% for the feedstock use and industrial production subsectors[24]. For the solvent/cleaning agent subsector, CH_3Br was assumed to be completely emitted within two years (50% in each year)[58] (see Supplementary Table 11).

In terms of combustion sector, we estimated the CH_3Br emissions from two combustion subsectors: open biomass burning and indoor biofuel burning[59]. For the open biomass burning subsector, we used dry matter burned mass data from the Global Fire Assimilation System (GFAS) database[60] and emission factors of six biomass types from Andreae[59]. The emission factor of each grid was determined by the corresponding gridded land-use and biomass types. Global land-use data were obtained from the MODIS satellite-derived product, MCD12C1. The global gridded CH_3Br emissions from open biomass burning were calculated by multiplying the dry matter burned mass matrix and the emission factor matrix (Eq. 6). Detailed information regarding this method is available in our previous study[61]. The emission factors for each biomass type are listed in Supplementary Table 12. For the indoor biofuel burning subsector, CH_3Br emissions

were calculated by multiplying the burned indoor agricultural residue mass by the emission factor. The burned indoor agricultural residue masses were equal to the product of the collected agricultural residue masses, grass-to-grain ratio of each crop, dry matter ratio of each crop residue, and burning ratio of the indoor biofuel[62]. We calculated the CH_3Br emissions from the indoor burning of the 15 main crops in China (Supplementary Table 13). Detailed information regarding the aforementioned parameters is provided in Supplementary Tables 13 and 14. The emission factor of burning for each crop was set at 0.0011 g kg^{-1} during the study period[59]. The detailed calculation formulas are as Eqs. (6–8):

$$E_{biomass\ burning,i,j,t} = DM_{i,j,t} \times Area_{i,j} \times EF_{i,j} \quad (6)$$

$$E_{indoor\ biofuel,t} = M_t \times EF_{indoor\ biofuel} \quad (7)$$

$$M_t = \sum_m P_{m,t} \times R_m \times r \times \sigma_{dry-matter} \times \varphi \quad (8)$$

$E_{biomass\ burning,i,j,t}$ is the emissions (kg s^{-1}) from biomass burning (open) of the grid (i,j) in year t, $DM_{i,j,t}$ is the dry matter burned mass (kg m^{-2} s^{-1}) of the grid (i,j) in year t, $Area_{i,j}$ is the area (m^2) of the grid (i,j), and $EF_{i,j}$ is the emission factor (g kg^{-1}) of the grid (i,j). $E_{indoor\ biofuel,t}$ denotes the emissions (Gg yr^{-1}) from indoor biofuel burning in year t, M_t is the total mass (kg yr^{-1}) of agricultural residue burned indoors in year t, and $P_{m,t}$ is the annual production (kg yr^{-1}) of crop m in year t, as taken from the China Rural Statistical Yearbook[63]. R_m is the grass-to-grain ratio (%) of the crop m, r is the burning ratio (%) of indoor burning, $\sigma_{dry-matter}$ is the dry matter ratio (%) of each crop residue, and φ is the combustion efficiency (%) of the indoor burning. The parameters of R_m, r, and $\sigma_{dry-matter}$ can be found in our previous study[62]. $EF_{indoor\ biofuel}$ is the emission factor (g kg^{-1}) of indoor biofuel burning.

In terms of terrestrial ecosystem sector, we included five terrestrial ecosystem emission subsectors (rice paddies[4,13,22], rapeseed[38,64], salt marshes[12,15], mangroves[4,11], and fungi (decomposition of dead litter))[4,27] in our bottom-up inventory. We extrapolated China's CH_3Br emissions from estimates of the planting areas for these sources[12,15,17]. For the rice paddy subsector, the emissions equal to China's rice planting area multiplied by the unit area emission flux (1.1 mg m^{-2}) obtained from Redeker et al.[22]. Data on China's rice-planting areas were obtained from the China Rural Statistical Yearbook[63] (Supplementary Table 15). For the rapeseed subsector, emissions were calculated as the global total emissions from rapeseed (2.8 Gg yr^{-1} in 2018[64]) multiplied by the ratio of China's rapeseed planting area to the global total planting area. The rapeseed planting areas in China and global totals were obtained from the China Rural Statistical Yearbook[63] (Supplementary Table 15) and the Food and Agriculture Organization (FAO, https://www.fao.org/faostat/en/#data/QCL/visualize), respectively. We scaled the corresponding global total sectoral emissions reported by WMO for salt marshes (7 (0.6–14) Gg yr^{-1})[4] and for mangroves (1.3 (1.2–1.3) Gg yr^{-1})[4] to China using the ratio of China's salt marsh (3.8×10^{11} m^2)[15] and mangrove (2.0×10^{11} m^2)[11] areas to global total areas. The salt marsh and mangrove area data for China were obtained from Chen et al.[65] and Wang et al.[66], respectively, and are presented in Supplementary Table 16. For the fungi subsector, we roughly assumed that the decomposition mass was proportional to the vegetation area; thus, we calculated China's CH_3Br emissions from fungi decomposition activities by multiplying global fungi emissions (2.2 (1–5.7) Gg yr^{-1})[4] and the ratio of China's vegetation area to global vegetation area calculated by the MODIS MCD12C1 product (https://ladsweb.modaps.eosdis.nasa.gov/archive/allData/6/MCD12C1/). The equations used for the calculations are as Eqs. (9–13):

$$E_{rice\ paddies,t} = A_{rice,t} \times F_{methyl\ bromide} \quad (9)$$

$$E_{rapeseed,t} = E_{global\ rapeseed,t} \times A_{China\ rapeseed,t} / A_{global\ rapessed,t} \quad (10)$$

$$E_{salt\ marsh,t} = E_{global\ salt\ marsh} \times A_{China\ salt\ marsh,t} / A_{global\ salt\ marsh} \quad (11)$$

$$E_{mangrove,t} = E_{global\ mangrove} \times A_{China\ mangrove,t} / A_{global\ mangrove} \quad (12)$$

$$E_{fungi,t} = E_{global\ fungi} \times A_{China\ vegetation,t} / A_{global\ vegetation,t} \quad (13)$$

$E_{rice\ paddies,t}$ is the emission (Gg yr^{-1}) from the rice paddies subsector in the year t, $A_{rice,t}$ is China's rice planting area (m^2) in the year t, $F_{methyl\ bromide}$ is the emission flux (mg m^{-2}) of CH_3Br from the rice paddies, $E_{rapeseed,t}$ the emission (Gg yr^{-1}) from the rapeseed subsector in the year t. $E_{global\ rapeseed,t}$ is the global emission (Gg yr^{-1}) from the rapeseed subsector in the year t, $A_{China\ rapeseed,t}$ and $A_{global\ rapeseed,t}$ are rapeseed planting areas (ha; 1 ha = 0.01 km^2)) of China and global totals in the year t. $E_{salt\ marsh,t}$ is the emission (Gg yr^{-1}) from the salt marsh subsector in the year t, and $A_{China\ salt\ marsh,t}$ and $A_{global\ salt\ marsh,t}$ are salt marsh areas (m^2) of China and global totals in the year t, respectively. $E_{mangrove,t}$ is the emission (Gg yr^{-1}) from the mangrove subsector in the year t, and $A_{China\ mangrove,t}$ and $A_{global\ mangrove,t}$ are mangrove areas (m^2) of China and global totals in the year t, respectively. $E_{fungi,t}$ is the emission from the fungi subsector in the year t, and $A_{China\ vegetation,t}$ and $A_{global\ vegetation,t}$ are vegetation areas (m^2) of China and global totals in the year t, respectively.

In this study's bottom-up inventory estimation, a normal distribution with 10% uncertainty for CH_3Br production and consumption data derived from our survey report[25]; a 5% uncertainty was adopted for all national statistical activity data (i.e., agricultural residue mass and rapeseed and rice cultivation areas) used in this study[58]. A Monte Carlo method with 100,000 samples was employed to calculate bottom-up emissions and uncertainties[58].

Metric for ozone depletion

A key metric to assess the ability of a compound to deplete stratospheric ozone is ODP, which is calculated relative to a reference compound (CFC-11 with an ODP of 1). We calculated the ODP-weighted emissions (CFC-11-equivalent emission) of CH_3Br by multiplying the mass emissions of CH_3Br by its ODP value. Additionally, we calculated integrated ozone depletion (IOD) to quantify the extra ozone depletion resulting from China's missing source during 2011–2050, assuming that the missing source (5.5 Gg yr^{-1} on average from 2011 to 2020) remains constant during 2021–2050. The time-integrated column ozone depletion can be calculated using halocarbon emissions and their total atmospheric and stratospheric lifetimes[67], as shown in Eq. (14):

$$IOD = K\,E_{Eq}\left(\frac{\tau_{atmos}}{\tau_{strat}}\right) \quad (14)$$

Here, $K = 100 \pm 16DU$ years per Tg Cl. E_{Eq} is the emissions in Tg Cl, and we multiplied a bromine efficiency factor of 60 to calculate E_{Eq} for CH_3Br[67]. τ_{atmos} and τ_{strat} are total atmospheric lifetime and stratospheric lifetime of CH_3Br.

Data availability

The emission sensitivity data sets generated in this study have been deposited in Figshare (https://figshare.com/s/2528c02b80e0f117ff2b). The CH_3Br measurement data for the AGAGE sites used in this study

are available at http://agage.mit.edu/data/agage-data. The Chinese and global CH_3Br QPS and non-QPS consumption data reported to the UNEP are available at https://ozone.unep.org/countries/. Global land-cover data for MCD12C1 are available at https://ladsweb.modaps.eosdis.nasa.gov/archive/allData/6/MCD12C1/. The global gridded dry matter burnt data of the GFASv1.2 database are available at https://apps.ecmwf.int/datasets/data/cams-gfas/. The agricultural residue mass data and Chinese national rice and rapeseed planting area data are available at http://www.stats.gov.cn/tjsj./ndsj/. Global cultivation area data for rice and rapeseed are available at https://www.fao.org/faostat/en/#data/QCL/visualize. Source data are provided with this paper.

Code availability

The code for the dispersion model FLEXPART is available at https://www.flexpart.eu.

References

1. Solomon, S., Garcia, R. R., Rowland, F. S. & Wuebbles, D. J. On the depletion of Antarctic ozone. *Nature* **321**, 755–758 (1986).
2. Polvani, L. M., Previdi, M., England, M. R., Chiodo, G. & Smith, K. L. Substantial twentieth-century Arctic warming caused by ozone-depleting substances. *Nat. Clim. Change* **10**, 130–133 (2020).
3. United Nations Environment Programme (UNEP). *Handbook For The Montreal Protocol On Substances That Deplete The Ozone Layer, T E*. (UNEP, 2009).
4. World Meteorological Organization (WMO). Scientific Assessment of Ozone Depletion: 2014. *Chapter 1: Update on Ozone-Depleting Substances (ODSs) and Other Gases of Interest to the Montreal Protocol*. (2014).
5. World Meteorological Organization (WMO). Scientific Assessment of Ozone Depletion: 2022. *Chapter 1: Update on Ozone-Depleting Substances (ODSs) and Other Gases of Interest to the Montreal Protocol*. (2022).
6. Methyl Bromide Technical Options Committee (MBTOC). *Methyl Bromide Technical Options Committee: Report of the Methyl Bromide Technical Options Committee: 2018 Assessment*, United Nations Environment Program, Nairobi, Kenya. https://ozone.unep.org/sites/default/files/2019-04/MBTOC-assessment-report-2018_1.pdf (UNEP, 2018).
7. Khalil, M. A. K., Rasmussen, R. A. & Gunawardena, R. Atmospheric methyl bromide: Trends and global mass balance. *J. Geophys. Res.: Atmos.* **98**, 2887–2896 (1993).
8. Hu, L., Yvon-Lewis, S., Liu, Y. & Bianchi, T. S. The ocean in near equilibrium with atmospheric methyl bromide. *Global Biogeochem. Cycles* **26** (2012).
9. Blake, N. J. et al. Biomass burning emissions and vertical distribution of atmospheric methyl halides and other reduced carbon gases in the South Atlantic region. *J. Geophys. Res.: Atmos.* **101**, 24151–24164 (1996).
10. Mano, S. & Andreae, M. O. Emission of methyl bromide from biomass burning. *Science* **263**, 1255–1257 (1994).
11. Manley, S. L., Wang, N.-Y., Walser, M. L. & Cicerone, R. J. Methyl halide emissions from greenhouse-grown mangroves. *Geophys. Res. Lett.* **34**, L01806 (2007).
12. Drewer, J., Heal, M. R., Heal, K. V. & Smith, K. A. Temporal and spatial variation in methyl bromide flux from a salt marsh. *Geophys. Res. Lett.* **33**, L16808 (2006).
13. Redeker, K. R., Andrews, J., Fisher, F., Sass, R. & Cicerone, R. J. Interfield and intrafield variability of methyl halide emissions from rice paddies. *Glob. Biogeochem. Cycles* **16**, 72-71–72-72-79 (2002).
14. Gan, J., Yates, S. R., Ohr, H. D. & Sims, J. J. Production of methyl bromide by terrestrial higher plants. *Geophys. Res. Lett.* **25**, 3595–3598 (1998).
15. Rhew, R. C., Miller, B. R. & Weiss, R. F. Natural methyl bromide and methyl chloride emissions from coastal salt marshes. *Nature* **403**, 292–295 (2000).
16. United Nations Environment Programme *(UNEP). Handbook for the Montreal Protocol on Substances That Deplete the Ozone Layer*, Twelfth edition. (United Nations Environment Programme (UNEP), Nairobi, Kenya, 2018). (2018).
17. Choi, H. et al. Top-down and bottom-up estimates of anthropogenic methyl bromide emissions from eastern China. *Atmos. Chem. Phys.* **22**, 5157–5173 (2022).
18. Li, S. et al. Emissions of halogenated compounds in East Asia determined from measurements at Jeju Island, Korea. *Environ. Sci. Technol.* **45**, 5668–5675 (2011).
19. Kim, J. et al. Regional atmospheric emissions determined from measurements at Jeju Island, Korea: Halogenated compounds from China. *Geophys. Res. Lett.* **37**, L12801 (2010).
20. Wang, C. et al. Estimating halocarbon emissions using measured ratio relative to tracers in China. *Atmos. Environ.* **89**, 816–826 (2014).
21. Fang, X. et al. Changes in Emissions of Ozone-Depleting Substances from China Due to Implementation of the Montreal Protocol. *Environ. Sci. Technol.* **52**, 11359–11366 (2018).
22. Redeker, K. R. et al. Emissions of methyl halides and methane from rice paddies. *Science* **290**, 966–969 (2000).
23. O'Doherty, S. et al. In situ chloroform measurements at Advanced Global Atmospheric Gases Experiment atmospheric research stations from 1994 to 1998. *J. Geophys. Res.: Atmos.* **106**, 20429–20444 (2001).
24. Intergovernmental Panel on Climate Change (IPCC). *2019 Refinement to the 2006 IPCC Guidelines for National Greenhouse Gas Inventories. Chapert 3: Chemical Industry Emissions*. (IPCC, 2019).
25. ASKCI. Report on bromomethanes industry in China (in Chinese). https://www.askci.com/reports/ (2021).
26. Lewis, R. A. *Hawley's Condensed Chemical Dictionary*, 12th Ed., New York, Van Nostrand Reinhold. 759 (1993).
27. Drewer, J., Heal, K. V., Smith, K. A. & Heal, M. R. Methyl bromide emissions to the atmosphere from temperate woodland ecosystems. *Glob. Change Biol.* **14**, 2539–2547 (2008).
28. Moore, R. M., Gut, A. & Andreae, M. O. A pilot study of methyl chloride emissions from tropical woodrot fungi. *Chemosphere* **58**, 221–225 (2005).
29. People's court of Anqiu City. A First instance criminal judgment of illegal business (in Chinese). https://www.lawtime.cn/caipan/1292254.html (2015).
30. Ministry of Ecology and Environment of the People's Republic of China. The Ministry of Environmental Protection announced the handling of key environmental cases in October 2014 (in Chinese). https://www.mee.gov.cn/gkml/sthjbgw/qt/201411/t20141117_291515_wh.htm (2014).
31. Ministry of Ecology and Environment of the People's Republic of China. The Ministry of Environmental Protection announced the handling of key environmental cases in August 2014 (in Chinese). https://www.gov.cn/foot/site1/20140929/782bcb888c4d15934c8201.pdf (2014).
32. People's Court of Shandong Province. First instance criminal judgment of illegal business (in Chinese). https://susong.tianyancha.com/3328c9f9a18d4fe3a9d2a258472075b4 (2016).
33. People's court of Anqiu City. First instance criminal judgment of illegal business (in Chinese). https://susong.tianyancha.com/e258227bdc66420b8c7915daa704f7eb (2016).
34. Aiqicha. Legal document of illegal business operation crime (in Chinese). https://aiqicha.baidu.com/nwenshu?wenshuId=01f0479a572a266cd4cc8b0cb0222c27c6967937 (2016).
35. Sohu. Four men were prosecuted in Rizhao on suspicion of illegal trafficking of drug products, environmental pollution and

counterfeiting of registered trademarks (in Chinese). https://www.sohu.com/a/519602203_121123881. (2022).
36. Sohu. A fine of 100,000! Lizin this aging fertilizer plant inside (in Chinese). https://www.sohu.com/a/439647511_670376 (2020).
37. Wishkerman, A. et al. Abiotic methyl bromide formation from vegetation, and its strong dependence on temperature. *Environ. Sci. Technol.* **42**, 6837–6842 (2008).
38. Mead, M. I., White, I. R., Nickless, G., Wang, K.-Y. & Shallcross, D. E. An estimation of the global emission of methyl bromide from rapeseed (Brassica napus) from 1961 to 2003. *Atmos. Environ.* **42**, 337–345 (2008).
39. Hu, L., Yvon-Lewis, S. A., Liu, Y., Salisbury, J. E. & O'Hern, J. E. Coastal emissions of methyl bromide and methyl chloride along the eastern Gulf of Mexico and the east coast of the United States. *Glob. Biogeochem. Cycles* **24**, GB1007 (2010).
40. Ministry of Ecology and Environment of the People's Republic of China. *Bulletin of Environmental Quality in China's coastal waters (in Chinese)*. https://www.mee.gov.cn/hjzl/sthjzk/jagb/ (2002).
41. Thornton, B. F., Horst, A., Carrizo, D. & Holmstrand, H. Methyl chloride and methyl bromide emissions from baking: an unrecognized anthropogenic source. *Sci. Total Environ.* **551-552**, 327–333 (2016).
42. Jiao, Y. et al. Application of copper(II)-based chemicals induces CH_3Br and CH_3Cl emissions from soil and seawater. *Nat. Commun.* **13**, 47 (2022).
43. Rigby, M. et al. Increase in CFC–11 emissions from eastern China based on atmospheric observations. *Nature* **569**, 546–550 (2019).
44. Park, S. et al. A decline in emissions of CFC-11 and related chemicals from eastern China. *Nature* **590**, 433–437 (2021).
45. Wu, J. et al. Banks, emissions, and environmental impacts of China's ozone depletion substances and hydrofluorocarbon substitutes during 1980-2020. *Sci. Total Environ.* **882**, 163586 (2023).
46. United States Environmental Protection Agency (US EPA). *Puerto Rico Pesticides Distributors Agree To Come into Compliance with Federal Law and Provide Training To Settle Case Involving Illegal Sale of Methyl Bromide Pesticides In Puerto Rico and the U.S. Virgin Islands*. https://www.epa.gov/archive/epa/newsreleases/puerto-rico-pesticides-distributors-agree-come-compliance-federal-law-and-provide-1.html (2016).
47. United Nations Environment Programme (UNEP). Training Manual for customs and enforcement officers (third edition). 50 (2013).
48. Fang, X. et al. Changes in HCFC Emissions in China During 2011–2017. *Geophys. Res. Lett.* **46**, 10034–10042 (2019).
49. Yao, B. et al. China's Hydrofluorocarbon Emissions for 2011–2017 Inferred from Atmospheric Measurements. *Environ. Sci. Technol. Lett.* **6**, 479–486 (2019).
50. Zhang, G. et al. Ambient mixing ratios of atmospheric halogenated compounds at five background stations in China. *Atmos. Environ.* **160**, 55–69 (2017).
51. An, M. et al. Rapid increase in dichloromethane emissions from China inferred through atmospheric observations. *Nat. Commun.* **12**, 7279 (2021).
52. Miller, B. R. et al. Medusa: a sample preconcentration and GC/MS detector system for in situ measurements of atmospheric trace halocarbons, hydrocarbons, and sulfur compounds. *Anal. Chem.* **80**, 1536–1545 (2008).
53. Fang, X. et al. Rapid increase in ozone-depleting chloroform emissions from China. *Nat. Geosci.* **12**, 89–93 (2018).
54. Stohl, A. et al. An analytical inversion method for determining regional and global emissions of greenhouse gases: Sensitivity studies and application to halocarbons. *Atmos. Chem. Phys.* **9**, 1597–1620 (2009).
55. Eckhardt, S. et al. Revised historical Northern Hemisphere black carbon emissions based on inverse modeling of ice core records. *Nat. Commun.* **14**, 271 (2023).
56. Sherry, D., McCulloch, A., Liang, Q., Reimann, S. & Newman, P. A. Current sources of carbon tetrachloride (CCl_4) in our atmosphere. *Environ. Res. Lett.* **13**, 024004 (2018).
57. Feng, Y., Bie, P., Wang, Z., Wang, L. & Zhang, J. Bottom-up anthropogenic dichloromethane emission estimates from China for the period 2005–2016 and predictions of future emissions. *Atmos. Environ.* **186**, 241–247 (2018).
58. Intergovernmental Panel on Climate Change (IPCC). *2006 IPCC Guidelines for National Greenhouse Gas Inventories, Volume 3: Industrial process and produc use*. (IPCC, 2006).
59. Andreae, M. O. Emission of trace gases and aerosols from biomass burning – an updated assessment. *Atmos. Chem. Phys.* **19**, 8523–8546 (2019).
60. Kaiser, J. W. et al. Biomass burning emissions estimated with a global fire assimilation system based on observed fire radiative power. *Biogeosciences* **9**, 527–554 (2012).
61. Hu, X. et al. Global methyl halide emissions from biomass burning during 2003-2021. *Environ. Sci. Ecotechnol.* **14**, 100228 (2023).
62. Hu, X., Yao, B. & Fang, X. Anthropogenic emissions of ozone-depleting substance CH_3Cl during 2000–2020 in China. *Environ. Pollut.* **310**, 119903 (2022).
63. National Bureau Of Statistics (NBS). China Rural Statistical Yearbook 2000-2020 (in Chinese) http://www.stats.gov.cn/tjsj./ndsj/ (China Statistics Press, 2020).
64. Jiao, Y. et al. Global Methyl Halide Emissions From Rapeseed (Brassica napus) Using Life Cycle Measurements. *Geophys. Res. Lett.* **47**, e2020GL089373 (2020).
65. Chen, G. et al. Spatiotemporal Mapping of Salt Marshes in the Intertidal Zone of China during 1985–2019. *J. Remote Sens.* **2022**, 9793626 (2022).
66. Wang, Z., Liu, K., Cao, J., Peng, L. & Wen, X. Annual Change Analysis of Mangrove Forests in China during 1986–2021 Based on Google Earth Engine. *Forests* **13**, 1489 (2022).
67. Pyle, J. A., Keeble, J., Abraham, N. L., Chipperfield, M. P. & Griffiths, P. T. Integrated ozone depletion as a metric for ozone recovery. *Nature* **608**, 719–723 (2022).

Acknowledgements

We acknowledge E. Saltzman (University of California, Irvine, California, USA) and A. R. Ravishankara (Colorado State University, Fort Collins, Colorado, USA) for their advice, comments, and revision of this paper. This work was supported by the National Natural Science Foundation of China (42277084) and National Key Research and Development Program of China (2019YFC0214500). AGAGE was supported by NASA grants to the Massachusetts Institute of Technology and the Scripps Institution of Oceanography. We further acknowledge the Level-1 and Atmosphere Archive & Distribution System (LAADS) Distributed Active Archive Center (DAAC) for archiving the global land cover data of MCD12C1, the Copernicus Atmosphere Monitoring Service for archiving the global gridded dry matter burnt data of the Global Fire Assimilation System (GFASv1.2) database, and the Advanced Global Atmospheric Gases Experiment (AGAGE) for archiving the global monthly mean mole fraction data of atmospheric CH_3Br.

Author contributions

X.F. and X.H. were responsible for project design. X.H. and X.F. conducted inverse modeling and developed a bottom-up inventory. B.Y. provided measurement data from ten Chinese sites. J.M., S.O'D., and R.G.P. provided measurements from four AGAGE (Advanced Global Atmospheric Gases Experiment) background sites. X.H. wrote the manuscript with revisions from J.M., R.R., P.J.F., S.O'D., and R.G.P.

Competing interests

The authors declare no competing interests.

Additional information

Supplementary information The online version contains supplementary material available at https://doi.org/10.1038/s41467-024-53188-3.

Correspondence and requests for materials should be addressed to Bo Yao or Xuekun Fang.

Peer review information *Nature Communications* thanks Eric Saltzman, Rafael Fernandez and the other, anonymous, reviewer(s) for their contribution to the peer review of this work. A peer review file is available.